Journal of CO2 Utilization 83 (2024) 102802

Contents lists available at ScienceDirect

Journal of CO2 Utilization

journal homepage: www.elsevier.com/locate/jcou

Value-added recycling of waste concrete fines into alternative aggregates for river sand conservation

Renjie Zhou [a], Yunjie Luo [a], Mingfang Ba [b], Zihua Zhang [b], Jianghua Fang [c], Chi Sun Poon [d], Xiaoliang Fang [b,*]

[a] School of Material Science and Chemical Engineering, Ningbo University, Ningbo, Zhejiang, China
[b] School of Civil & Environmental Engineering and Geography Science, Ningbo University, Ningbo, Zhejiang, China
[c] School of Materials and Chemical Engineering, Ningbo University of Technology, Ningbo, Zhejiang, China
[d] Department of Civil and Environmental Engineering, The Hong Kong Polytechnic University, Hung Hom, Kowloon, Hong Kong

ARTICLE INFO

Keywords:
Fine recycled concrete aggregate
Wet carbonation
Waste upcycling
Chemical treatment
Low-carbon construction materials

ABSTRACT

Due to the depletion of river sand, the construction industry is eager to develop upcycling techniques for transforming secondary by-products derived from construction and demolition (C&D) waste into quality fine aggregates. This paper presents a study of replacing river sand with enhanced recycled fine aggregate through a wet carbonation process developed by the authors previously. The fine recycled concrete aggregate (FRCA) ranging from 0.15 to 5 mm was prepared by demolishing a concrete with a known mixture design. After wet carbonation, the particle size, water absorption, and density of the FRCA were tested and compared with the original samples. The chemical characteristics of the original and carbonated FRCA (C-FRCA) were analyzed by a series of experiments. The results showed that (1) an increase of carbonation products and a significant reduction of hydration products; (2) microscopic observation of the C-FRCA showed a surface layer densified by calcite after wet carbonation; and (3) no significant strength loss were observed when replacing up to 50% river sand by C-FRCA in mortar specimens. The potential environmental and economic impacts were also analyzed.

1. Introduction

Rapid urbanization made concrete the most widely used construction material worldwide. As the major fine aggregate of commercial ready-mix concrete, the natural river sand resource is therefore depleting [1,2]. On the other hand, the fine fraction of the recycled concrete aggregate derived from construction and demolition (C&D) waste lacks practical and economical approaches to transform it into value-added products due to a high content of adhered mortar [3–5].

Previous studies have been conducted on replacing river sand with various types of recycled aggregates [6–10]. Safi et al. used waste plastic (0.3–4 μm) as fine aggregate to replace river sand in mortar specimens. The compressive strength of the self-compacting mortar specimens was reduced from 20% to 50% for each plastic waste replacement [11]. Agrawal et al. utilized geopolymer fly ash sand (GFS) to replace river sand by preparing geopolymer sand particles with GFS and achieved a 28-day strength of 93.6% of that of natural river sand specimens [12]. Bhardwaj et al. described a technique of replacing natural fine aggregates with waste foundry sand (WFS) by analyzing its appearance, morphology, and performance. The strength of concrete specimens with a 100% WFS replacement ratio is about half of that prepared by NRS [13]. Santhosh et al. compared the effects of incorporating 15 types of industrial by-products as fine aggregates in concrete specimens [14]. The results show that steel slag, copper slag, Ferrochromium Slag (FCS), and granite dust samples achieved the best performance at a replacement ratio of 20% while bottom ash and crushed stone samples achieved a 40% replacement ratio. The optimal replacement ratio for ceramic and recycled glass was 60% and 10% respectively. Chandru et al. studied the effect of various fine aggregates recycled from C&D into plain concrete and Portland Pozzolana Cement (PPC) concrete [15]. The results showed that replacing 15%, 30%, 50%, and 100% of natural fine aggregate resulted in a reduction in compressive strength by 8.1%, 21.7%, 25.1%, and 28.6%, respectively. According to previous attempts, the incorporation of recycled fine aggregates usually led to a noticeable deterioration in concrete performance, and the replacement ratio was limited to below 50%.

On the other hand, sustainable development requires the construction industry to upcycle construction and demolition (C&D) waste into

* Corresponding author.
E-mail address: fangxiaoliang@nbu.edu.cn (X. Fang).

https://doi.org/10.1016/j.jcou.2024.102802
Received 8 December 2023; Received in revised form 29 February 2024; Accepted 6 May 2024
Available online 16 May 2024

Table 1
Mix proportion of the original concrete.

Unit(kg/m3)	OPC	Water	Sand	5–10 mm aggregate	10–20 mm aggregate
	460	205	700	530	430

Table 2
Cement content of FRCA.

Particle size (mm)	0.15–0.3	0.3–0.6	0.6–1.18	1.18–2.36	2.36–5
Cement content (%)	33.77 ±1.69	27.71 ±1.39	25.51 ±1.28	23.59 ±1.18	23.28 ±1.16

Table 3
Particle size distribution of river sand.

Particle size (mm)	0.15–0.3	0.3–0.6	0.6–1.18	1.18–2.36	2.36–5
passing	36.10%	55.56%	6.23%	1.19%	0.92%

value-added products. But using recycled concrete aggregate (RCA) directly in concrete leads to a significant reduction in its performance due to the porous adhered mortar and the weak interface transition zone [16]. Accelerated carbonation is considered one of the most effective and practical approaches to enhance the quality of RCA. However, the carbonation enhancement for FRCA was limited due to the high content of adhered mortar.

To further enhance the quality of the FRCA, attempts were made to improve the carbonation effect of FRCA [17]. Pan et al. utilized calcium hydroxide to soak FRCA before CO_2 curing procedures [18]. After the carbonation process, the powder content, water absorption and crush value of the FRCA were reported decreased by 5.1%, 2.7%, and 5%, respectively. And the compressive strength of the mortar samples made with C-FRCA was increased by 26%. Hence, the externally added calcium significantly increased the carbonation products and effectively improved the quality of the FRCA after carbonation. Li et al. studied the internal curing effect of the mortar prepared with saturated FRCA [19]. Utilizing saturated FRCA was reported beneficial for compensating autogenous shrinkage of mortar specimens prepared with FRCA. Shi et al. employed a granulation technique to produce artificial aggregates with 5–20 mm particle size by using RCA below 5 mm [20]. After carbonation treatment, the produced artificial aggregates showed property enhancement and construction application potential. Zhang et al. improved the prediction model of RAC carbonation depth by

Table 4
Composition ratio table of nine groups of mortar specimens (kg/m^3).

Aggregate type	River sand replacement ratio	Cement	Water	River sand	FRCA	C-FRCA
River sand	0%	800	400	2400	0	0
FRCA	25%	800	400	1800	600	0
	50%	800	400	1200	1200	0
	75%	800	400	600	1800	0
	100%	800	400	0	2400	0
C-FRCA	25%	800	400	1800	0	600
	50%	800	400	1200	0	1200
	75%	800	400	600	0	1800
	100%	800	400	0	0	2400

Table 5
Adjusted water usage.

Aggregate type	River sand replacement ratio	Adjusted water usage (g)
River sand	0%	25.7
FRCA	25%	34.1
	50%	36.2
	75%	53.1
	100%	58.9
C-FRCA	25%	32.3
	50%	35.6
	75%	45.6
	100%	48.4

Table 6
Density and water absorption of FRCA and C-FRCA samples.

Particle size (mm)	Density (kg/m^3)		Water absorption (%)	
	FRCA	C-FRCA	FRCA	C-FRCA
0.15–0.3	2265.6 ±68.0	2907.6±90.1	61.19 ±3.06	30.00 ±1.50
0.3–0.6	2365.9 ±94.6	2900.9 ±101.5	50.97 ±2.55	32.36 ±1.62
0.6–1.18	2317.7 ±74.2	2466.6±81.4	36.54 ±1.83	25.79 ±1.29
1.18–2.36	2212.6 ±59.4	2820.8 ±141.0	26.39 ±1.32	18.66 ±0.93
2.36–5	2467.1 ±74.0	2687.0±53.7	17.75 ±0.89	11.33 ±0.57

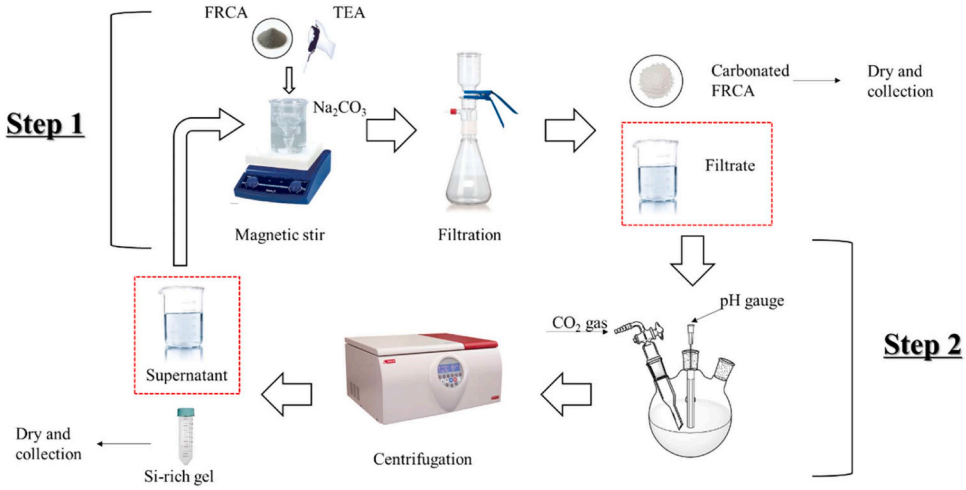

Fig. 1. Illustration of the wet carbonation process [32].

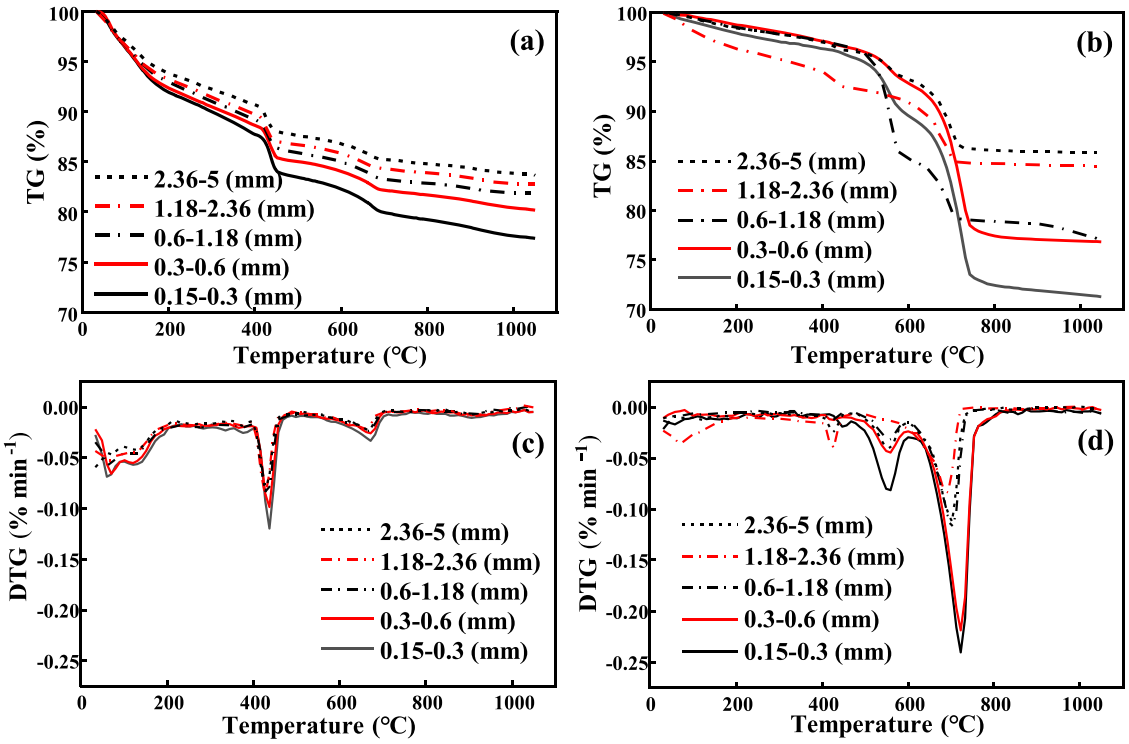

Fig. 2. (a) TG of FRCA; (b) TG of C-FRCA; (c) DTG of FRCA; (d) DTG of C-FRCA.

Table 7
Content of CH and CC by TGA.

Particle size (mm)	CH (wt%)		CC (wt%)	
	FRCA	C-FRCA	FRCA	C-FRCA
0.15–0.3	24.49	3.87	11.89	64.69
0.3–0.6	20.40	4.29	9.05	51.55
0.6–1.18	19.02	3.61	7.88	36.42
1.18–2.36	17.55	3.49	7.26	31.75
2.36–5	17.24	5.13	7.16	22.91

Table 8
XRF results of the C-FRCA.

Oxidation	Unit: wt%				
	0.15–0.3 (mm)	0.3–0.6 (mm)	0.6–1.18 (mm)	1.18–2.36 (mm)	2.36–5 (mm)
CaO	64.40	64.90	52.00	38.40	42.90
SiO_2	22.80	25.40	37.80	41.00	41.70
Al_2O_3	3.000	2.550	2.580	3.66	3.910
Fe_2O_3	1.850	1.490	1.700	1.480	2.690
SO_3	0.079	0.063	0.152	0.037	0.218
MgO	1.390	1.250	1.200	1.170	1.690
K_2O	0.522	0.571	0.611	0.580	0.797
TiO_2	0.279	0.249	0.194	0.246	0.459
Na_2O	1.270	0.919	0.937	1.820	1.410
P_2O_5	0.097	0.073	0.079	0.080	0.159
MnO	0.122	0.101	0.086	0.072	0.082
SrO	0.133	0.106	0.087	0.075	0.085
Cr_2O_3	N/A	N/A	N/A	N/A	0.011
ZnO	0.006	0.007	0.004	0.004	0.012
NiO	N/A	0.005	N/A	0.004	0.008
F	4.1	2.3	2.5	11.4	3.9

introducing the weighing water absorption of the aggregates to reduce the coefficient of variation (COV) of the existing models [21]. Xiao et al. found that the carbon emission of recycled concrete with recycled powder decreased by 12.4–52.2% compared to normal concrete [22].

Table 9
Mass of Si-rich gel from Step 2.

Particle size (mm)	0.15–0.3	0.3–0.6	0.6–1.18	1.18–2.36	2.36–5
Gels (g)	0.8784	0.6830	0.6309	0.6104	0.4295

Utilizing saturated FRCA was reported beneficial for compensating autogenous shrinkage of mortar specimens prepared with FRCA. Wang et al. reviewed the existing literature on applications of carbonation of cement-based materials in the past two decades [23]. The carbonated calcium was reported up to about 75% and the reduced water absorption ranged from 7.6% to 54.2%. The authors also pointed out that the efficiency of carbonation can be improved by optimizing through parameter adjustment. Therefore, the potential of CO_2 sequestration by carbonation of cement-based recycled materials is huge.

Recently, a two-step wet carbonation method was developed by transforming conventional gas-solid carbonation into a liquid-solid state. With this method, efficient carbonation recycling of old cement paste powder was achieved [24,25]. In contrast to previous accelerated carbonation treatment, the wet carbonation was modified to conduct liquid-solid phase carbonation [26]. In this way, a solution rich in carbonate ions (CO_3^{2-}) was able to react directly with the hydration products to produce carbonation products, which result in a relatively higher carbonation efficiency. This method managed to collect calcium-rich carbonation products and silicon-rich carbonation products separately [27,28]. After collecting the precipitated calcium carbonate, CO_2 gas was introduced into the solution to precipitate a silica-rich gel and to replenish the CO_3^{2-} depleted in the solution, allowing it to be recycled. Therefore, the developed wet carbonation method showed great potential in both river sand conservation, solid waste mitigation and CO_2 absorption by transforming FRCA into fine aggregate.

Even though wet carbonation was able to enhance the carbonation reaction, the wet carbonation currently published utilized crushed cement paste to produce fine particles instead of real FRCA sourced from concrete [29–31]. This study aims to utilize the developed wet carbonation method to treat FRCA ranging from 0.15 to 5 mm and reuse

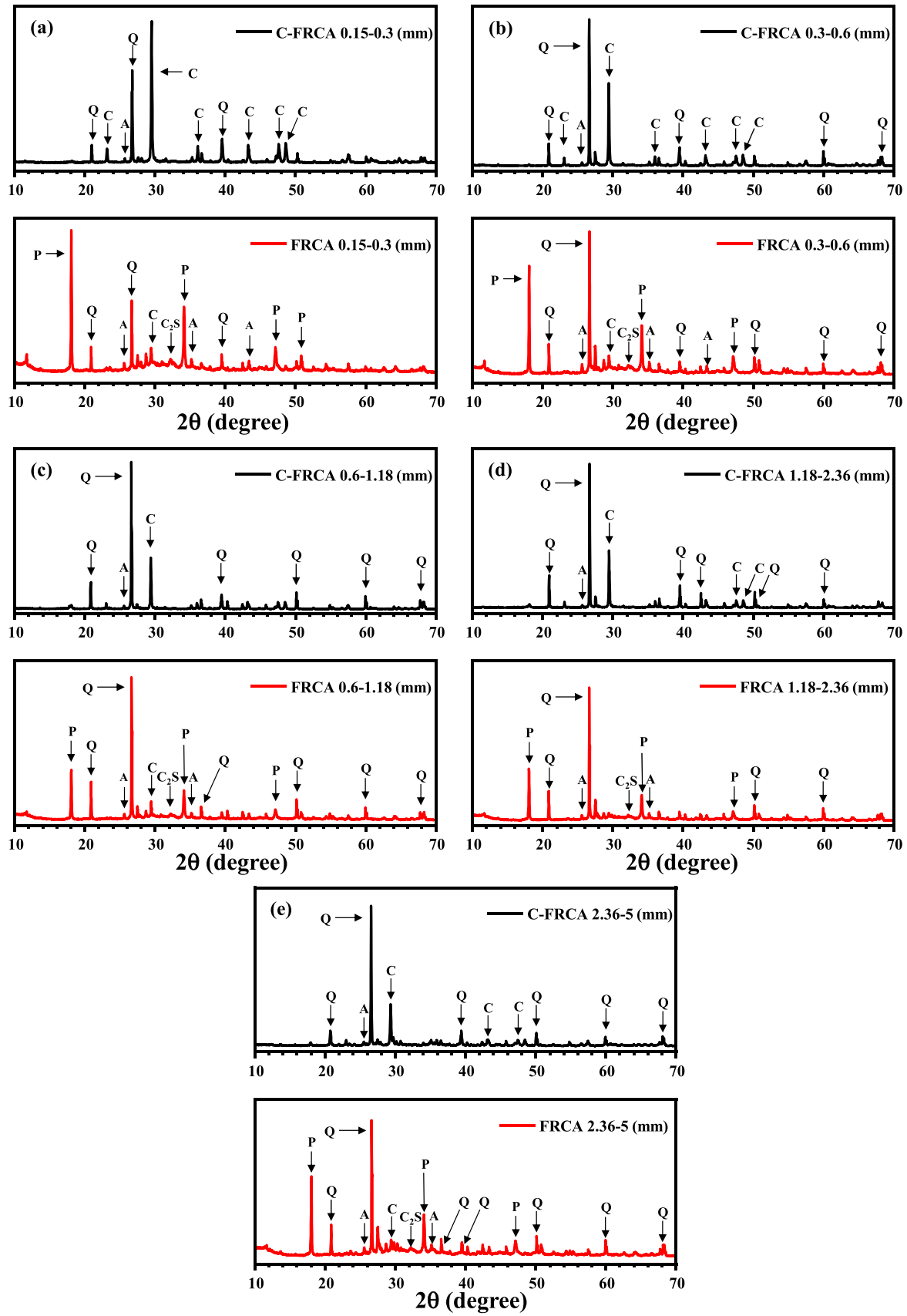

Fig. 3. XRD patterns of FRCA and C-FRCA: (a) a particle size range of 0.15–0.3 mm; (b) a particle size range of 0.3–0.6 mm; (c) a particle size range of 0.6–1.18 mm; (d) a particle size range of 1.18–2.36 mm; (e) a particle size range of 2.36–5 mm. (A = corundum; P = portlandite; Q = quartz; C = calcite; C_2S = dicalcium silicate).

Table 10
Content of CH and CC by semi-QXRD.

Particle size (mm)	CH (wt%)		CC (wt%)	
	FRCA	C-FRCA	FRCA	C-FRCA
0.15–0.3	47.96	0.36	11.97	41.08
0.3–0.6	30.35	0.35	7.75	30.16
0.6–1.18	29.01	0.79	9.75	27.26
1.18–2.36	29.19	0.85	3.89	26.45
2.36–5	27.66	1.21	7.34	21.89

the carbonated FRCA to replace river sand in mortar specimens. The density and water absorption of FRCA were compared before and after the carbonation. The chemical composition and the microscopic changes of FRCA were observed and compared. The mechanical property of the mortar specimens prepared with FRCA and river sand were tested and compared.

2. Materials and methods

2.1. Carbonation methods

A solution of 5% Na_2CO_3 was prepared by weighing 950 g of deionized water and 50 g of anhydrous Na_2CO_3 powder. FRCA was added at a solid-to-liquid ratio of 1:100 and 0.5 wt% of triethanolamine (TEA) was added as a catalyst. The mixture was stirred using a magnetic stirrer at 500 r/min for 24 h under room temperature. The Ca-rich residue and supernatant were obtained by filtration. The Ca-rich residue was washed three times with deionized water to remove the Na^+ and then dried at 105℃. The supernatant was injected by a CO_2 gas (purity>99.9%) at a flow rate of 5 L/min controlled by a gas flow meter. The pH value was monitored by a pH meter. When the pH value was below 9.80, the Si-rich gel was washed and collected by centrifugation.

2.2. Materials

2.2.1. FRCA

The FRCA used in this study was derived from crushing a concrete with a known mixture proportion listed in Table 1. The original concrete was designed with an effective water/cement ratio of 0.45 and cement of 460 kg/m^3. The cement used to prepare the original concrete was a type 53.5R commercial cement provided by a local factory. At the age of 1 month, the concrete was crushed to produce RCA which was sieved, collected, and stored in air-tight bags afterward for 1 year before the test. The FRCA was further sieved into 5 groups with a particle size of 0.15–0.3 mm, 0.3–0.6 mm, 0.6–1.18 mm, 1.18–2.36 mm, and 2.36–5 mm, respectively. The cement content was measured and calculated by using 10% hydrochloric acid as the dissolution agent. The cement content of the FRCA was listed in Table 2.

A commercial river sand provided by local manufacturer was used as reference in this study. The sieve analysis of the river sand is shown in Table 3.

2.2.2. Chemical agent

The setup of wet carbonation was described in a previous study (Fig. 1) [32,33]. In step 1, the Na_2CO_3 solution was used to react with the hydration products remaining in the adhered mortar, and the silica was precipitated by a CO_2 gas in step 2. The solid products of step 1 and step 2 were collected by filtration and centrifugation, respectively. Both samples were oven dried for 24 h at 105℃ before testing. The information of the chemical agents used in this test was listed as follows:

2.2.2.1. Na_2CO_3 solution. A Na_2CO_3 solution was prepared through dissolving an AR-grade Na_2CO_3 powder in deionized water. The concentration of Na_2CO_3 solution was 0.5 mol/L according to the previous study. Triethanolamine (TEA) was added into the Na_2CO_3 solution (0.5 wt%), serving as a chelating agent for Ca^{2+}.

2.2.2.2. CO_2 gas. The CO_2 gas was commercially sourced with a purity of > 99.9%.

2.2.3. Mortar specimens

Mortar specimens were prepared with an ASTM type I ordinary Portland cement (OPC), three types of fine aggregate: river sand, FRCA, and carbonated FRCA (C-FRCA). A compressive strength test (ASTM C349–08,2008) was conducted to compare the effects of replacing river sand with both FRCA and C-FRCA. The effective water-to-cement ratio and the cement-to-aggregate ratio of the mortar specimens were 0.5 and 1:3 respectively (Table 4). It should be noted that for the mixtures, water was adjusted in order to reach the same flowability (ASTM C1437). The adjusted amount of water was shown in Table 5. For each group of mortar mixture, three 40 mm×40 mm×40 mm cubes were prepared respectively.

2.3. Testing methods

2.3.1. Density and water absorption

In order to be consistent with the previous study [33], the density and water absorption of FRCA and C-FRCA samples were measured according to BS EN 1097 [34].

2.3.2. Particle size

The particle size of C-FRCA was obtained through a sieve analysis by using a GB/T6003.1–1997 standard sieve set. After the sieve analysis, the particles larger than 0.15 mm were re-collected for testing. After wet carbonation, the same sieve analysis was conducted and the particles smaller than 0.15 mm was collected and measured.

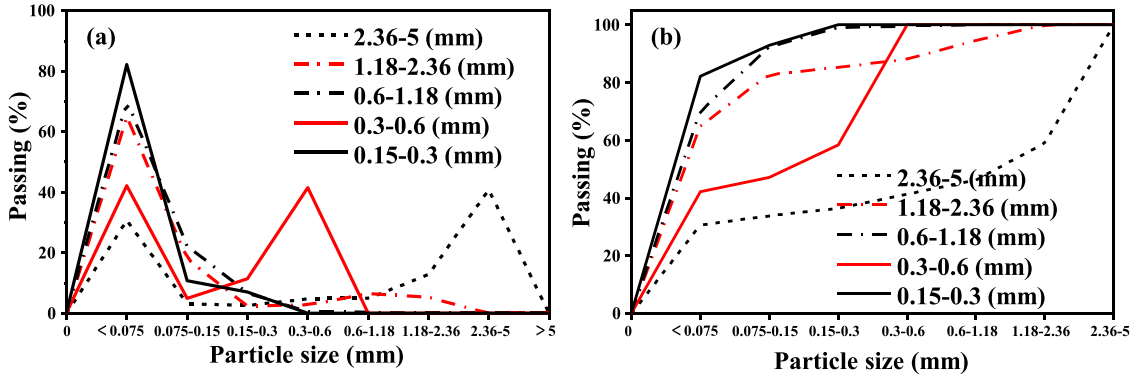

Fig. 4. Particle size distribution of C-FRCA: (a) distributional and (b) cumulative.

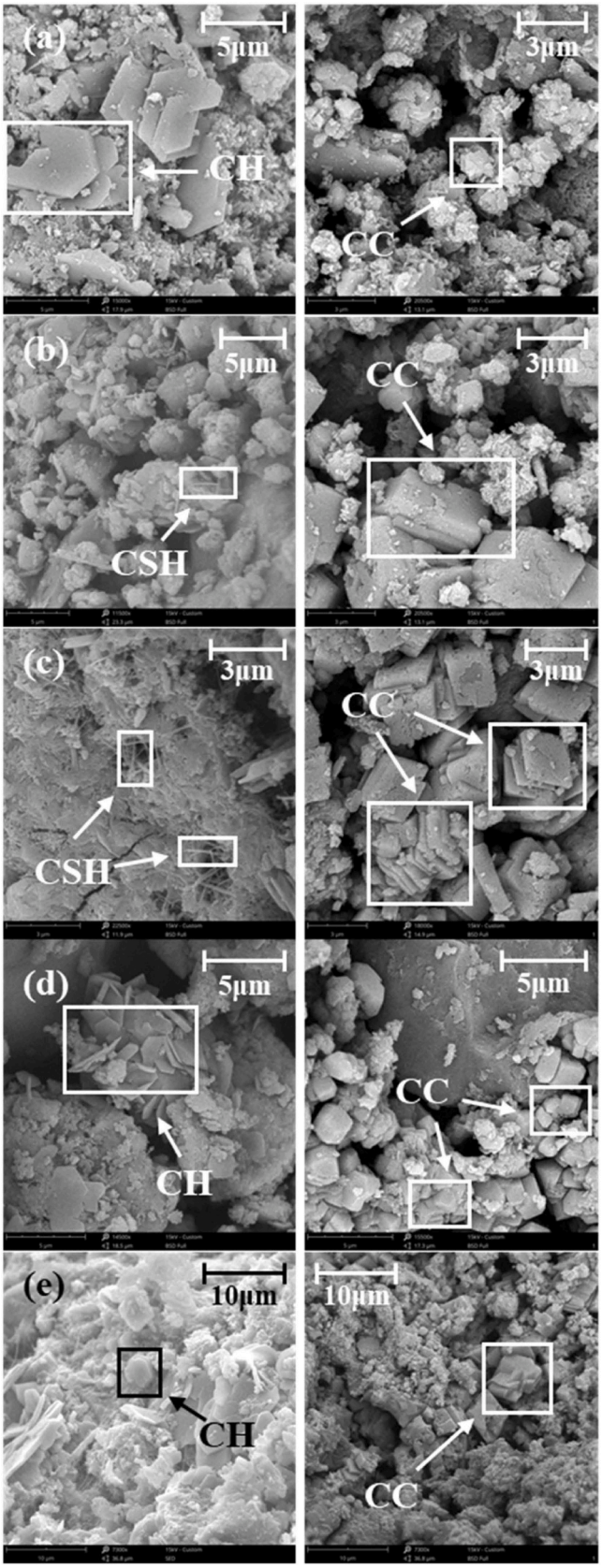

Fig. 5. SEM images of FRCA and C-FRCA: (a) a particle size range of 0.15–0.3 mm; (b) a particle size range of 0.3–0.6 mm; (c) a particle size range of 0.6–1.18 mm; (d) a particle size range of 1.18–2.36 mm; (e) a particle size range of 2.36–5 mm. (FRCA on the left; C-FRCA on the right).

Table 11
EDS data of CH and CC.

CH		CC	
Element	Mass %	Element	Mass %
O	49.63	O	72.78
Ca	50.37	Ca	27.22

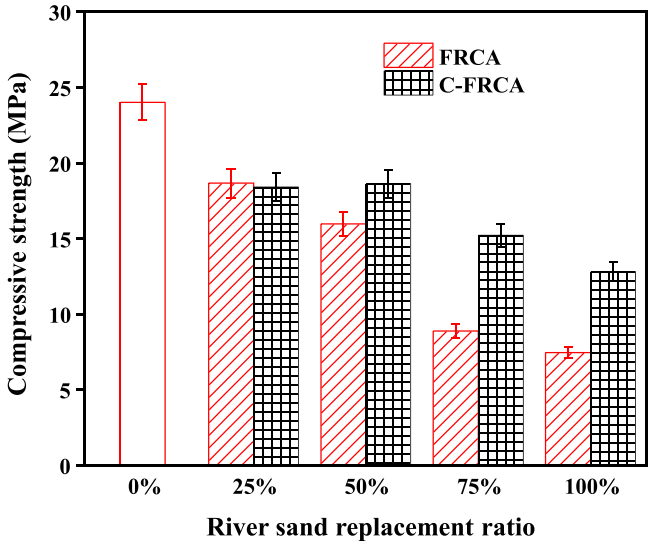

Fig. 6. Compressive strength of mortar specimens.

2.3.3. Thermogravimetric analysis (TGA)

The solid samples used for the XRF, TGA, XRD, and SEM were dried powders (at 60°C for 24 h) and were ground to pass through a 75-micron sieve.

TGA was conducted by a Nissan STA2500 using nitrogen as the protective gas. TGA of the samples was conducted to measure the mass of the samples at 1050ºC. The fraction of both hydration and carbonation products can be calculated by mass loss between 350 and 450ºC and 550–850ºC. The sample was measured between 40 and 1050°C with an increment of 10°C per minute. The formulae for calculating CC and CH content are listed as follows:

$$m_{CH} = \left(\Delta m_{350-450} \div Mr_{H_2O} \times Mr_{Ca(OH)_2}\right) \div m_{1050} \times 100\%$$

$$m_{CC} = \left(\Delta m_{550-850} \div Mr_{CO_2} \times Mr_{CaCO_3}\right) \div m_{1050} \times 100\%$$

Where, m_{CH} and m_{cc} are the mass of CH and CC respectively; $\Delta m_{350-450}$and $\Delta m_{550-850}$ are the measured mass loss between two temperature range respectively; m_{1050} is the ignited residue mass of the sample; and Mr_{H_2O}, Mr_{CO_2}, Mr_{CaCO_3}, and $Mr_{Ca(OH)_2}$ are the molar mass of H_2O, CO_2, CC and CH respectively.

2.3.4. Microscopic analysis

XRD was conducted by a (BRUKER) D8 Advance model at an operating power of 40kw and 40 mA. 10% corundum (Al_2O_3) was incorporated into the samples for a semi-quantitative analysis by using the RIR method [35]. The samples were scanned over a range of 10–70º, with a step size of 0.02º and a scanning speed of 5º per minute.

XRF was performed by using a (BRUKER) model S8 TIGER to analyze the oxide compositions of both the FRCA samples and the C-FRCA samples. The solid samples were prepared by a briquette method using boric acid as the binder.

The scanning electron microscope (SEM) utilized a COXEM EM-30AX$^+$ with secondary electronic signal to obtain the characteristics of the carbonation products at the microscopic level.

Table 12
Comparison of the carbonation effect for FRCA.

Treatment methods	FRCA type	Properties of treated FRCA			Source(s)
		Enhancement ratio of density (%)	Water absorption (%)	Carbonation products (CC)	
10 min fast water carbonation	0.15–0.6 mm	N/A	N/A	+3.5%	Fang et al. [37]
	0.6–1.18 mm			+3.3%	
	1.18–2.36 mm			+2.8%	
	2.36–5 mm			+2.6%	
CO_2 curing after CH pre-soaking	<4.75 mm	N/A	-2.35	N/A	Pan et al. [18]
20% CO_2 chamber	0.16–0.315 mm	+4.74/+5.62	-2.28/-1.97	+7.9%	Zhang et al. [38]
	0.315–0.63 mm			+7.6%	
	0.63–1.25 mm			+5.2%	
	1.25–2.5 mm			+2.9%	
Two-step wet carbonation	0.15–0.3 mm	+28.34	-31.9	+36.9%	Current study
	0.3–0.6 mm	+22.61	-18.6	+32.3%	
	0.6–1.18 mm	+6.42	-10.8	+21.6%	
	1.18–2.36 mm	+27.49	-7.7	+9.8%	
	2.36–5 mm	+8.91	-6.4	+13.7%	

Table 13
Rough estimates of annual economic gains by the wet carbonation process for a local construction firm.

Annual FRCA treatment capability: 37,500 ton		
Disposal of C&D waste and consumption of river sand	Two-step carbonation (estimation)	
Gains	Cost	Gains
■ Avoided landfill disposal cost: US$ 1.0M ■ Saved river sand cost: US$ 0.85 M	■ Energy: US$ 0.04M ■ Cyclically used $Na_{2CO3:\ US\$\ 0.35M}$ ■ Operating cost of treatment plant: US $ 0.4 M	■ C-FRCA sale: US$ 0.23M ■ Government subsidy: US $ 0.08M ■ 16,110 tons of $CaCO_3$ with market value of US$ 8.06M ■ About 7500 tons of Si-rich gel with further potential value

3. Results and discussion

3.1. Profiles of solid products

Table 6 shows the density and water absorption values of FRCA and C-FRCA samples with different particle size ranges before and after the wet carbonation process. All C-FRCA samples showed an increased density and reduced water absorption after the wet carbonation process. C-FRCA with the smallest particle size (0.15–0.3 mm) showed a 28.3% increment in density and a 47.9% reduction in water absorption value while the largest C-FRCA particles showed 8.9% and 36.2%, respectively. It is noticed that the property enhancement ratio of C-FRCA with particle size smaller than 0.6 mm was significant, suggesting an effective transformation of hydration products into carbonation products and a densified particle. Meanwhile, C-FRCA with larger particle size showed less increase in density values which was possibly due to the relatively lower mortar content and the precipitation of carbonation products [36]. As FRCA with a larger particle size contains more large pores which led to a precipitation of carbonation products into solutions, the density of the density of the 2.36–5 mm C-FRCA was lower than those fractions with smaller particle sizes. Nevertheless, the presence of CC in C-FRCA particles would benefit the hydration of the new cement paste and the strength development of the mortar specimens [26]. On the other hand, the water absorption value halved for the finest group of C-FRCA after wet carbonation, while larger particles showed relatively less reduction. The possible reason is that some adhered mortar reacted with the solution and dissolved during the wet carbonation process, canceling the pore-filling effect of the produced solid carbonation products, especially for large particles owing to larger pore sizes. The reduced water absorption value indicated a denser surface of C-FRCA after wet carbonation. Even though the water absorption value of C-FRCA was significantly lowered, it was still slightly above that of river sand. On the upside, a slightly higher water absorption value might contribute to the strength development of its mortar specimens through internal curing effect.

3.2. Carbonation products

The TG and DTG results of both FRCA and C-FRCA are presented in Fig. 2. The contents of portlandite (CH) and calcium carbonate (CC) were calculated and listed in Table 7. The DTG curves show a substantial increase in the content of CC and a significant reduction of the content of CH in C-FRCA samples compared with the FRCA, indicating that wet carbonation effectively transformed the soluble CH into solid CC. The data in Table 7 shows that 0.15–0.3 mm C-FRCA contained more CH owing to a higher cement content and more CC due to a relatively higher natural carbonation rate caused by small particle size. After wet carbonation, the CH content of C-FRCA groups with particle size ranging from 0.15 to 2.36 mm reduced to a comparable level from 3.49% to 4.29%. Meanwhile the 2.36–5 mm C-FRCA showed a higher CH content possibly due to a relatively lower reaction rate and more non-carbonated inner areas. The mass loss peak at about 410°C indicated that CH were remaining in C-FRCA. It is due to the fast densification at the surface layer of the adhered mortar of FRCA during the carbonation process. On the other hand, C-FRCA samples smaller than 1.18 mm showed a higher CC content than those larger than 1.18 mm after wet carbonation. Thus, it is noticed that a smaller particle size results in a lower content of CH and a higher content of CC owing to a higher carbonation efficiency [36]. Besides, C-FRCA with smaller particle sizes also showed a higher content of remaining CH, suggesting that wet carbonation was also limited by the densified surface area of the adhered mortar [36]. The value of CC content also revealed that the wet carbonation using Na_2CO_3 is more effective than using water as a previous study showed [37].

3.3. Chemical composition

Table 8 presents the XRF results of the mass fractions of each chemical composition in the form of oxides. It is noticed that the mass fraction of CaO reduced as the particle size increased. The possible reason is that more calcite particles were precipitated into the solution during step 1 as the calcite particles were more difficult to remain in a larger pore system in the adhered mortar under a high-speed stir condition. Meanwhile, the increased SiO_2 content in larger C-FRCA particles was probably the result of i) a higher river sand content in larger C-FRCA particles and ii) less carbonated C-S-H owing to a lower reaction rate. Table 9 shows the mass of gel collected from Step 2 reduces as the particle size increases owing to a lower mortar content and a slower carbonation reaction rate. It should be noted that the chemical

composition of the Si-rich gel was same as previous study [33]. The findings indicated that the carbonation efficiency of C-S-H was reduced as the particle size of FRCA increased.

Fig. 3 shows the XRD patterns of FRCA and C-FRCA samples. The XRD pattern revealed a significant increase in the peak intensity of calcite after wet carbonation. It is also noticed that the peak of quartz dominated after wet carbonation except the 0.15–0.3 mm C-FRCA, implying a reduction of adhered mortar content in C-FRCA. For 0.15–0.3 mm samples, the content of calcite was higher than the content of quartz due to a higher content of hydration products. The contents of CH and CC calculated by semi-quantitative XRD are listed in Table 10. Similar to the TG results, a reduction in CH content and an increase in CC content were observed. According to Table 10, the remaining CH in C-FRCA was less than 2% after wet carbonation, suggesting a high carbonation efficiency. Meanwhile, the semi-QXRD also showed a smaller CC value because only crystalline phase of CC can be measured by XRD. The CC content of the 2.36–5 mm C-FRCA was the lowest possibly owing to a low mortar content and the loss of calcite in solution due to a larger pore size according to previous study [37].

3.4. Particle size distribution

Fig. 4 presents the (a) distributional and (b) cumulative curves of C-FRCA particle size after wet carbonation. Fig. 4(a) reveals all C-FRCA samples showed an increase in particles smaller than 0.075 mm which were mainly solid carbonation products (e.g. calcite). FRCA with a smaller particle size produced more carbonation products as discussed previously. Fig. 4(b) indicates a reduced average particle size of C-FRCA after wet carbonation, indicating the disintegration of the adhered mortar and the production of carbonation products due to the decomposition and carbonation of hydration products. It is also interestingly observed that 1.18–2.36 mm and 2.36–5 mm C-FRCA still containing about 10% and 40% large particles respectively. The reason is that the produced carbonation products which filled the pore area would not be measured by the particle size analysis [37].

3.5. Microscopic observation

Fig. 5 shows the microscopic images of FRCA and C-FRCA. Hydration products, mainly CH and C-S-H were noticed at the surface of FRCA particles before wet carbonation. Also, there were voids between the loosely packed CH and CSH. After carbonation, carbonation products, mainly calcite, were noticed packed densely at the same location of the C-FRCA particles, indicating the surface layer was effectively densified through pore-filling effect by the wet carbonation process [36]. There were hardly any hydration products observed at the surface layer after wet carbonation, which suggested that both CH and CSH were carbonated during the process. Besides, silica gel was not observed after wet carbonation as it dissolved into the solution at a high pH condition. The SEM observation agrees with the chemical analysis results of the content change of both hydration and carbonation products before and after the wet carbonation. The densified surface also explained the remaining CH content as it would prevent CO_3^{2-} from permeating into inner layers of the adhered mortar [36]. The EDS data of CH and CC in Table 11 agrees that the microscopic observation provided solid evidence that the FRCA particles were densified effectively by wet carbonation.

3.6. Application in mortar specimens

According to Fig. 6, the control specimen prepared with 100% river sand achieved the highest compressive strength while the specimen prepared with 100% FRCA achieved the lowest owing to an inferior property of FRCA. The compressive strength decreases as the FRCA replacement ratio increases. Replacing 25% and 50% river sand by C-FRCA resulted in similar strength values. While a significant strength reduction was observed when 50–75% of river sand was replaced by uncarbonated FRCA. But replacing 75% river sand by C-FRCA showed much less strength reduction. Moreover, the specimens prepared with C-FRCA only showed a 71.85% strength enhancement compared with those prepared with FRCA only, due to the produced carbonation products that would benefit the interface between C-RFA and the cement paste [26]. In addition, the higher water absorption might result in a better internal curing effect to compensate for the strength loss. The results suggested that the wet carbonation effectively improved the quality of FRCA and compensated strength loss especially when over 50% river sand was replaced. Therefore, the developed two-step wet carbonation approach was able to enhance the mechanical performance of mortar specimens by improving the quality of FRCA.

3.7. Comparison with previous studies

Table 12 shows the comparison between different treatment methods for improving the quality of FRCA. The effect of wet carbonation utilizing Na_2CO_3 is better than conventional carbonation chamber, enhanced accelerated carbonation, and water carbonation. Both the carbonation chamber and enhanced accelerated carbonation reduced the water absorption of FRCA by less than 3% while the current study managed to reduce water absorption of FRCA by more than 6%. Furthermore, the wet carbonation of the current study produced significantly more carbonation products (CC) than all the previous methods. Thus, the two-step wet carbonation provided an effective approach for improving the quality of FRCA.

3.8. Potential environmental and economic impacts

Table 13 showed the rough estimation of the potential economic impact of utilizing wet carbonation for a local construction firm with a daily RCA treatment capability of 1000 tons. As the local statistics suggested RCA contains a 15 wt% content of FRCA, the annual FRCA production would be 37,500 tons (250 working days). Therefore, if the FRCA can be recycled, it would have an economic gain of US$ 1.0 M as avoided landfill disposal cost. Moreover, due to the shortage of supply, the price of river sand is US$ 22.76 per ton. Theoretically, utilizing C-FRCA as the substitution for river sand would save up to US$ 0.85 M.

On the other hand, the price of industrial grade Na_2CO_3 and $CaCO_3$ is about US$ 200 and US$ 500 per ton respectively (Alibaba). Therefore, the estimated annual cost of the cyclically used Na_2CO_3 would be US$ 0.35 M. The annual energy and operation cost of the wet carbonation process would be US$ 0.04 M and US$ 0.4 M respectively. As the profit of C-FRCA is US$ 6 per ton, the annual C-FRCA profit would be US$ 0.23 M. According to the lab data, the 37,500 tons of C-FRCA would generate 16,110 tons of $CaCO_3$ which value at least US$ 8.06 M. In addition, the government subsidy (i.e. mainland China) for recycling RCA is US$ 2 per ton, which results in an annual subsidy of US$ 0.08 M. Meanwhile, the Si-rich gel is also potentially valuable as it can be used as SCMs or raw materials for producing nano silica [39]. Moreover, the C-FRCA with improved properties can be utilized in more value-added products, which also benefits the upscaling of the RCA recycling industry.

The CO_2 absorption was calculated according to the CC content in Table 10 (XRD). The CO_2 absorption of the FRCA groups from small to large particle size was 16.2%, 14.2%, 9.5%, 4.3%, and 6.0%, respectively. Accordingly, the amount of CO_2 absorbed by river sand grade FRCA was 136 kg per ton. Similarly, according to the CC content in Table 7 (TGA), the CO_2 absorption FRCA was 131 kg per ton.

4. Conclusions

In order to study the effect of a two-step wet carbonation method on enhancing the quality of FRCA with a particle size range of 0.15–5 mm, a series of experimental investigations were conducted. Both the physical and chemical properties of FRCA particles were examined and compared

before and after wet carbonation treatment. The conclusions can be drawn as follows:

The quality of FRCA was significantly enhanced by wet carbonation, evidenced by the increased density of up to 28.3% and reduced water absorption of up to 47.9%.

The content of CH in C-FRCA can be reduced to less than 5% after wet carbonation while the content of CC can be significantly increased to over 40%. The mass fraction of quartz increased after wet carbonation except for 0.15–0.3 mm particles;

The particle size was generally reduced due to the precipitation of carbonation products in the solution;

After wet carbonation, the voids near the surface of the C-FRCA particles were filled by carbonation products, and the original hydration products were mostly carbonated.

The application of wet carbonation resulted in a 71.85% increase in the compressive strength of mortar specimens prepared by C-FRCA. Replacing up to 50% river sand by C-FRCA would not result in significant performance deterioration.

To sum up, the wet carbonation developed by the cement powder test can be effectively utilized to enhance the quality of FRCA.

CRediT authorship contribution statement

ZHOU Renjie:Conceptualization, Methodology, Investigation, Data analysis, Writing–original draft, Writing–review&editing. **LUO Yunjie**: Conceptualization, Methodology, Writing–review & editing. **BAMing fang**: Methodology, Writing–review & editing. **ZHANG Zihua**:Conceptualization, Methodology. **FANG Jianghua**: Laboratory management, Supervison. **POONChi Sun**: Writing- review&editing. **FANG Xiaoliang**: Conceptualization, Supervision, Methodology, Writing – review &f inalizing.

Declaration of Competing Interest

The authors certify that they have NO affiliations with or involvement in any organization or entity with any financial interest or non-financial interest in the subject matter or materials discussed in this manuscript.

Data availability

Data will be made available on request.

Acknowledgments

This work was supported by Ningbo Municipal Natural Science Foundation (2022J082), Ningbo University (NBU 42221823), and The Hong Kong Polytechnic University.

References

[1] Z. Zhang, Z. Zhang, S. Yin, L. Yu, Utilization of iron tailings sand as an environmentally friendly alternative to natural river sand in high-strength concrete: shrinkage characterization and mitigation strategies, Materials 13 (2020) 1–15, https://doi.org/10.3390/ma13245614.

[2] H. Song, G. Gu, Y. Cheng, Experimental study on river sand replacement in concrete, IOP Conf. Ser. Earth Environ. Sci. (2020), https://doi.org/10.1088/1755-1315/567/1/012013.

[3] V. Revilla-Cuesta, M. Skaf, F. Faleschini, J.M. Manso, V. Ortega-López, Self-compacting concrete manufactured with recycled concrete aggregate: an overview, J. Clean. Prod. 262 (2020), https://doi.org/10.1016/j.jclepro.2020.121362.

[4] Q. Li, J. Hu, Mechanical and durability properties of cement-stabilized recycled concrete aggregate, Sustainability 12 (2020), https://doi.org/10.3390/SU12187380.

[5] W. Zhu, J. Wang, L. Wang, M. Ying, X. Hu, H. Fu, Effect of particle distribution on the shear behavior of recycled concrete aggregate, Arab. J. Geosci. 15 (2022), https://doi.org/10.1007/s12517-022-10166-7.

[6] A.G. Pillai, M.L. Gali, Engineering benefits of replacing natural sand with manufactured sand in landfill construction, Sci. Rep. 13 (2023) 6444, https://doi.org/10.1038/s41598-023-32835-7.

[7] K. Sundaralingam, A. Peiris, A. Anburuvel, N. Sathiparan, Quarry dust as river sand replacement in cement masonry blocks: effect on mechanical and durability characteristics, Materialia 21 (2022), https://doi.org/10.1016/j.mtla.2022.101324.

[8] B.C. Lyu, L.P. Guo, X.P. Fei, J.D. Wu, R.S. Bian, Preparation and properties of green high ductility geopolymer composites incorporating recycled fine brick aggregate, Cem. Concr. Compos. 139 (2023), https://doi.org/10.1016/j.cemconcomp.2023.105054.

[9] V. Letelier, M. Bustamante, P. Muñoz, S. Rivas, J.M. Ortega, Evaluation of mortars with combined use of fine recycled aggregates and waste crumb rubber, J. Build. Eng. 43 (2021), https://doi.org/10.1016/j.jobe.2021.103226.

[10] C. Fang, J. Feng, S. Huang, J. Hu, W. Wang, N. Li, Mechanical properties and microscopic characterization of mortar with recycled aggregate from waste road, Case Stud. Constr. Mater. 17 (2022), https://doi.org/10.1016/j.cscm.2022.e01441.

[11] B. Safi, M. Saidi, D. Aboutaleb, M. Maallem, The use of plastic waste as fine aggregate in the self-compacting mortars: effect on physical and mechanical properties, Constr. Build. Mater. 43 (2013) 436–442, https://doi.org/10.1016/j.conbuildmat.2013.02.049.

[12] U.S. Agrawal, S.P. Wanjari, D.N. Naresh, Characteristic study of geopolymer fly ash sand as a replacement to natural river sand, Constr. Build. Mater. 150 (2017) 681–688, https://doi.org/10.1016/j.conbuildmat.2017.06.029.

[13] B. Bhardwaj, P. Kumar, Waste foundry sand in concrete: a review, Constr. Build. Mater. 156 (2017) 661–674, https://doi.org/10.1016/j.conbuildmat.2017.09.010.

[14] K.G. Santhosh, S.M. Subhani, A. Bahurudeen, Cleaner production of concrete by using industrial by-products as fine aggregate: a sustainable solution to excessive river sand mining, J. Build. Eng. 42 (2021), https://doi.org/10.1016/j.jobe.2021.102415.

[15] U. Chandru, A. Bahurudeen, R. Senthilkumar, Systematic comparison of different recycled fine aggregates from construction and demolition wastes in OPC concrete and PPC concrete, J. Build. Eng. 75 (2023), https://doi.org/10.1016/j.jobe.2023.106768.

[16] M. Barreto Santos, J. de Brito, A. Santos Silva, A. Hawreen, Effect of the source concrete with ASR degradation on the mechanical and physical properties of coarse recycled aggregate, Cem. Concr. Compos. 111 (2020), https://doi.org/10.1016/j.cemconcomp.2020.103621.

[17] V. Revilla-Cuesta, V. Ortega-López, M. Skaf, J.M. Manso, Effect of fine recycled concrete aggregate on the mechanical behavior of self-compacting concrete, Constr. Build. Mater. 263 (2020), https://doi.org/10.1016/j.conbuildmat.2020.120671.

[18] G. Pan, M. Zhan, M. Fu, Y. Wang, X. Lu, Effect of CO2 curing on demolition recycled fine aggregates enhanced by calcium hydroxide pre-soaking, Constr. Build. Mater. 154 (2017) 810–818, https://doi.org/10.1016/j.conbuildmat.2017.07.079.

[19] Z. Li, J. Liu, J. Xiao, P. Zhong, Internal curing effect of saturated recycled fine aggregates in early-age mortar, Cem. Concr. Compos. 108 (2020), https://doi.org/10.1016/j.cemconcomp.2019.103444.

[20] M. Shi, T.C. Ling, B. Gan, M.Z. Guo, Turning concrete waste powder into carbonated artificial aggregates, Constr. Build. Mater. 199 (2019) 178–184, https://doi.org/10.1016/j.conbuildmat.2018.12.021.

[21] K. Zhang, J. Xiao, Prediction model of carbonation depth for recycled aggregate concrete, Cem. Concr. Compos. 88 (2018) 86–99, https://doi.org/10.1016/j.cemconcomp.2018.01.013.

[22] J. Xiao, Y. Xiao, Y. Liu, T. Ding, Carbon emission analyses of concretes made with recycled materials considering CO2 uptake through carbonation absorption, Struct. Concr. 22 (2021) E58–E73, https://doi.org/10.1002/suco.201900577.

[23] D. Wang, J. Xiao, Z. Duan, Strategies to accelerate CO2 sequestration of cement-based materials and their application prospects, Constr. Build. Mater. 314 (2022), https://doi.org/10.1016/j.conbuildmat.2021.125646.

[24] J. Wang, M. Mu, Y. Liu, Recycled cement, Constr. Build. Mater. 190 (2018) 1124–1132, https://doi.org/10.1016/j.conbuildmat.2018.09.181.

[25] T. Li, J. Xiao, C. Zhu, Hydration process modeling of ITZ between new and old cement paste, Constr. Build. Mater. 109 (2016) 120–127, https://doi.org/10.1016/j.conbuildmat.2016.01.053.

[26] S. Liu, P. Shen, D. Xuan, L. Li, A. Sojobi, B. Zhan, C.S. Poon, A comparison of liquid-solid and gas-solid accelerated carbonation for enhancement of recycled concrete aggregate, Cem. Concr. Compos. 118 (2021), https://doi.org/10.1016/j.cemconcomp.2021.103988.

[27] J. Pei, R. Sharma, J.G. Jang, Use of carbonated Portland cement clinkers as a reactive or non-reactive aggregate for the production of cement mortar, Constr. Build. Mater. 319 (2022), https://doi.org/10.1016/j.conbuildmat.2021.126070.

[28] D. Suescum-Morales, K. Kalinowska-Wichrowska, J.M. Fernández, J.R. Jiménez, Accelerated carbonation of fresh cement-based products containing recycled masonry aggregates for CO2sequestration, J. CO2 Util. 46 (2021), https://doi.org/10.1016/j.jcou.2021.101461.

[29] M. Zajac, J. Skibsted, P. Durdzinski, F. Bullerjahn, J. Skocek, M. Ben Haha, Kinetics of enforced carbonation of cement paste, Cem. Concr. Res. 131 (2020), https://doi.org/10.1016/j.cemconres.2020.106013.

[30] M. Zajac, J. Skibsted, J. Skocek, P. Durdzinski, F. Bullerjahn, M. Ben Haha, Phase assemblage and microstructure of cement paste subjected to enforced, wet carbonation, Cem. Concr. Res. 130 (2020), https://doi.org/10.1016/j.cemconres.2020.105990.

[31] M. Zajac, A. Lechevallier, P. Durdzinski, F. Bullerjahn, J. Skibsted, M. Ben Haha, CO2 mineralisation of Portland cement: towards understanding the mechanisms of enforced carbonation, J. CO2 Util. 38 (2020) 398–415, https://doi.org/10.1016/j.jcou.2020.02.015.

[32] X. Fang, D. Xuan, B. Zhan, W. Li, C.S. Poon, Characterization and optimization of a two-step carbonation process for valorization of recycled cement paste fine powder, Constr. Build. Mater. 278 (2021), https://doi.org/10.1016/j.conbuildmat.2021.122343.
[33] X. Fang, D. Xuan, B. Zhan, W. Li, C.S. Poon, A novel upcycling technique of recycled cement paste powder by a two-step carbonation process, J. Clean. Prod. 290 (2021), https://doi.org/10.1016/j.jclepro.2020.125192.
[34] BSI Standards Publication Tests for mechanical and Physical Properties of Aggregates Part 6: Determination of Particle Density and Water Absorption, 2013.
[35] F.H. Chung, Quantitative Interpretation of X-ray Diffraction Patterns of Mixtures. I. Matrix-Flushing Method for Quantitative Multicomponent Analysis, 1974.
[36] M. Thiery, P. Dangla, P. Belin, G. Habert, N. Roussel, Carbonation kinetics of a bed of recycled concrete aggregates: a laboratory study on model materials, Cem. Concr. Res. 46 (2013) 50–65, https://doi.org/10.1016/j.cemconres.2013.01.005.
[37] X. Fang, D. Xuan, P. Shen, C.S. Poon, Fast enhancement of recycled fine aggregates properties by wet carbonation, J. Clean. Prod. 313 (2021), https://doi.org/10.1016/j.jclepro.2021.127867.
[38] J. Zhang, C. Shi, Y. Li, X. Pan, C.-S. Poon, Z. Xie, Performance enhancement of recycled concrete aggregates through carbonation, J. Mater. Civ. Eng. 27 (2015), https://doi.org/10.1061/(asce)mt.1943-5533.0001296.
[39] P. Shen, Y. Sun, S. Liu, Y. Jiang, H. Zheng, D. Xuan, J. Lu, C.S. Poon, Synthesis of amorphous nano-silica from recycled concrete fines by two-step wet carbonation, Cem. Concr. Res. 147 (2021) 106526, https://doi.org/10.1016/j.cemconres.2021.106526.